Modification of stainless steel based on synergistic of low-energy high-intensity ion implantation and high-current electron beam impact on the surface layer

A I Ryabchikov[1], **O S Korneva**[1], **D O Sivin**[1], **A I Ivanova**[1], **I V Lopatin**[2] **and I A Bozhko**[1]

[1] National Research Tomsk Polytechnic University, Tomsk, Russia
[2] Institute of High Current Electronics, Siberian Branch, Russian Academy of Sciences, Tomsk, Russia

E-mail: oskar@tpu.ru

Abstract. The results of experiments on low-energy implantation of AISI 321 stainless steel by nitrogen ions are presented. The treatment was carried out by a pulsed beam of nitrogen ions obtained using a ballistic ion focusing system. The surface modification occurs with the formation of a two-layer structure, which is typical for ion-plasma nitriding processes of stainless steels. The thickness of the modified layer can reach 27 μm after 1 hour of ion-plasma treatment. The influence of subsequent modification of the ion-doped layer by the action on the surface of the pulsed high-current electron beam of microsecond duration is studied. The work presents the results of the studying the regularities of changes in the depth distribution of dopants, microstructure and phase composition of the modified and matrix layers by optical metallography, diffraction analysis and transmission electron microscopy.

1. Introduction

Methods to saturate the surface of materials and products in a solid state with various doping elements are widely used in science and technology. One of the widespread approaches to changing the elemental and phase composition of the near-surface layer is ion-plasma methods of diffusion saturation [1-3], involving heating the workpiece to temperatures of 400–800°C, when added substance atoms' diffusion is intensified and provides modified layers with a thickness from tens to hundreds of micrometers per unit-tens of hours. The process of diffusion saturation of a surface with nitrogen atoms is called nitriding; it is widely used in industry [4-7]. It was shown in [8] that an increase in the ion current density intensifies the nitriding process. At the same time, increasing the ion energy up to several hundred electron volts, it is possible to carry out both efficient ion cleaning of the surface from oxides formed on it, and to implement their low-energy implantation [9]. To increase the pulsed and average ion current density, the system of ion beam ballistic focusing in a spherical configuration was proposed in [10, 11]. Experimental studies on high-intensity implantation of nitrogen ions into AISI 5140 steel have shown that due to radiation-enhanced diffusion at elevated temperature, a deep ion-doped layer is formed [12]. At the same time, high temperatures stimulate rapid grain growth.

In this work, it is proposed to study the combination of high-intensity nitrogen ion implantation into AISI 321 steel with post-implantation impact on the ion-doped layer of a high-current electron beam with sub-millisecond duration.

2. The experimental setup and methodology of the research

The nitrogen ion implantation into AISI 321 steel was carried out on an experimental setup with plasma-immersion extraction of ions and their subsequent ballistic focusing, described in detail in [13]. To form high-intensity beams of nitrogen ions, a repetitively-pulsed negative bias potential with an amplitude of 1.2 kV, pulse duration of 10-11 μs and a pulse repetition rate of 40 kHz, was applied to the focusing system. A cylindrical stainless grid with a radius of 130 mm had a cell size 1×1 mm^2. The ion beam formation system was located opposite a plasma generator PINK-P [14] with heated and hollow cathodes of an extended design with a length of 400 mm at a distance of 180 mm from the end of its hollow cathode.

Stainless AISI 321 steel was selected as the material for the study. Samples with sizes of 45×25×3 mm^3 after polishing and chemical cleaning were mounted on a collector located in the focal plane of the beam formation system. The samples' temperature was measured with an insulated chromel-alumel thermocouple installed on the sample's back side in its center.

Before the main modification process, the samples were cleaned and heated by argon ions with energy of 1.2 keV for 20 min. Nitrogen ions with an energy of 1.2 keV were implanted into stainless steel samples at an operating pressure of 0.6 Pa for 60 min at an arc discharge current of a PINK-P plasma generator of 25 A.

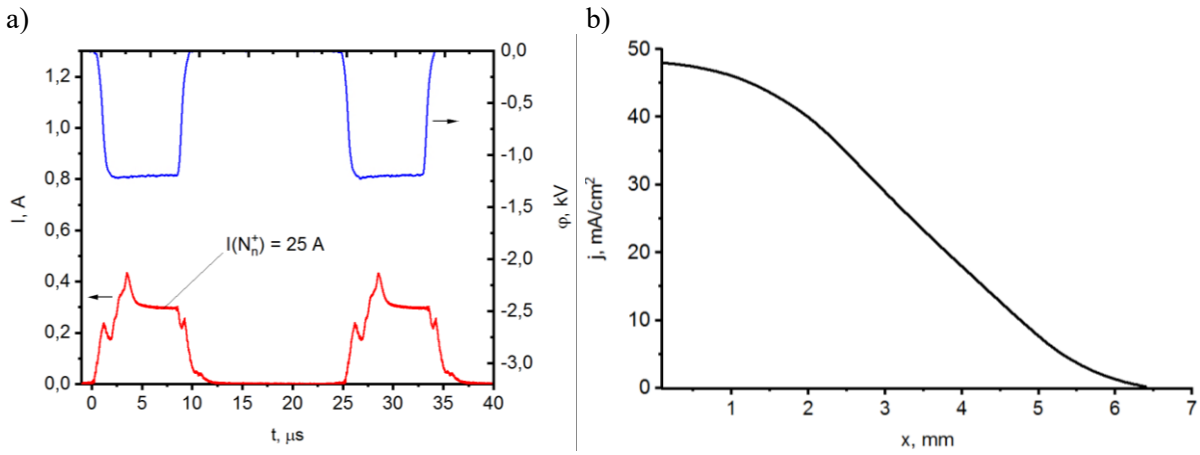

Figure 1. Oscillograms of the bias potential pulses and ion current to the collector during the nitrogen ion beams' formation, obtained at a discharge current of 25 A (a) and ion current density distribution over the beam cross section (b).

Figure 1 shows typical oscillograms of the nitrogen ion beam's current and voltage, and the current density distribution over the beam's cross section. After treatment, the samples were cooled in a working chamber to a temperature of less than 70°C at a pressure not higher than 5×10^{-2} Pa.

Subsequent exposure to a sub-millisecond intense low-energy electron beam on the sample's surface implanted with nitrogen ions was carried out using an electronic source "SOLO" [15]. The electron-beam treatment of the sample was carried out with an electron beam with a pulse duration of 20 μs in the single-pulse regime (the number of irradiation pulses was 5) with an energy density in the beam of 4 and 6 J/cm^2.

To carry out metallographic studies and determine the nitrogen distribution over the modified layer's thickness, transverse sections were made using a grinding and polishing machine "Saphir 320". For a clearer identification of the metallographic structure, the thin sections were etched in a mixture of nitric, hydrochloric acids and glycerol. Dopants' depth distribution along the sample was studied

using a Hitachi S-3400 N scanning electron microscope equipped with a Bruker XFlash 4010 energy dispersive X-ray attachment and a LEO EVO-50XVP scanning electron microscope with an INCA-Energy dispersive microanalyzer (Oxford Instruments). The phase composition of the nitrided layers was determined by X-ray structural analysis using a DRON-7 diffractometer. Diffraction patterns of the studied samples were recorded with continuous 2θ scanning with Bragg-Brentano focusing in radiation from a cobalt anode (radiation wavelength Co Kα $\lambda = 0.1789$ nm). The crystalline phases were identified using the "JCPDS PDF-2" database of the ICDD structural database. The microstructure was studied on a Philips CM 30 transmission electron microscope. Foils for studies by transmission electron microscopy were made according to the "cross-section" scheme by ion etching using an argon ion beam on an ION-SLICER EM-09100IS installation (JEOL).

3. Results and discussion

High-intensity low-energy nitrogen ion implantation into stainless steel was carried out when the sample temperature reached 500°C for one hour to a fluence of 4.3×10^{20} ion/cm^2. This treatment of stainless steel resulted in the formation of a two-layer structure with a total modified layer thickness of up to 27 μm. Figure 2a shows a micrograph of a metallographic section showing an ion-doped layer. Figure 2b shows the elemental mapping results.

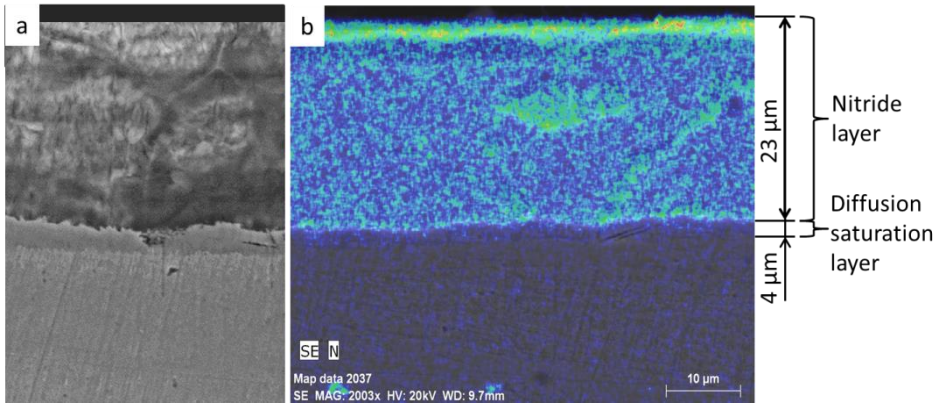

Figure 2. Metallographic thin section (a) and nitrogen distribution map (b) of the cross-section of a stainless steel sample implanted with nitrogen ions.

Figure 3 shows the graphs of nitrogen dopants' distribution over the implanted sample depth by nitrogen ions and subsequent exposure to an electron beam. As a result of high-intensity nitrogen ion implantation, an ion-doped layer with a thickness of about 27 μm with a nitrogen concentration of about 25 at.% was formed, and the profile of the dopant distribution has a plateau-like shape.

Exposure to a high-current electron beam transforms the distribution of nitrogen. The layer width decreases to 20 μm and at the same time the nitrogen concentration decreases to about 17 at.% at an electron beam energy density of 4 J/cm^2. An increase in the electron beam energy density to 6 J/cm^2 is accompanied by evaporation of the near-surface layer, which leads to a decrease in the thickness of the ion-doped layer, although the nitrogen concentration remains approximately the same as in the case of a lower electron beam energy density.

The data of X-ray phase analysis of a sample of AISI 321 steel in the initial state showed that the main phase is austenite (γ-Fe) with a lattice parameter $a = 3.5999$ Å. As a result of nitrogen ion implantation into austenitic AISI 321 steel at a temperature of 500°C, a surface-modified layer is formed, in which the iron nitride ε-Fe_3N formation is observed and a phase transition occurs $\gamma \geq \alpha$. At that, the volume fraction of the α-phase is 79.4 wt.%, and the γ-phase is 20.6 wt.%. It should be noted that the diffraction lines observed in the diffractograms of the studied samples have significant broadening. The observed broadening of the diffraction lines is due to the fact that the formed ε-Fe_3N

crystallites are small. This is confirmed by the results of determining the sizes of the coherent scattering regions (CSR) of the formed phases by the Selyakov-Scherrer method. Using the broadening of the most intense diffraction line (101), it was found that the CSR size for ε-Fe_3N is about 20 nm.

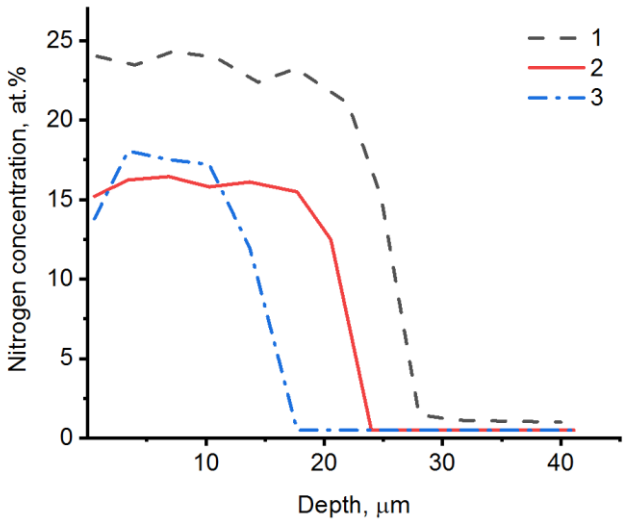

Figure 3. Nitrogen dopants' distribution over the depth of the sample after high intensity ion implantation and subsequent exposure to an electron beam: 1 - implanted sample, 2 - energy density in the electron beam of 4 J/cm^2, 3 – 6 J/cm^2.

Figure 4 shows the results of electron microscopic studies of the microstructure and phase composition of a stainless steel sample implanted with nitrogen ions in a cross section. The microdiffraction pattern contains high-intensity point matrix reflections, as well as point reflections with a lower intensity. The identification of this microdiffraction pattern showed that α-Fe matrix grains have a zone axis [111]. Point reflections with lower intensity, which are present in the microdiffraction pattern, belong to the high-nitrogen ε-phase Fe_3N (FCC), the particles of which have a zone axis $[\bar{3}1\bar{1}]$.

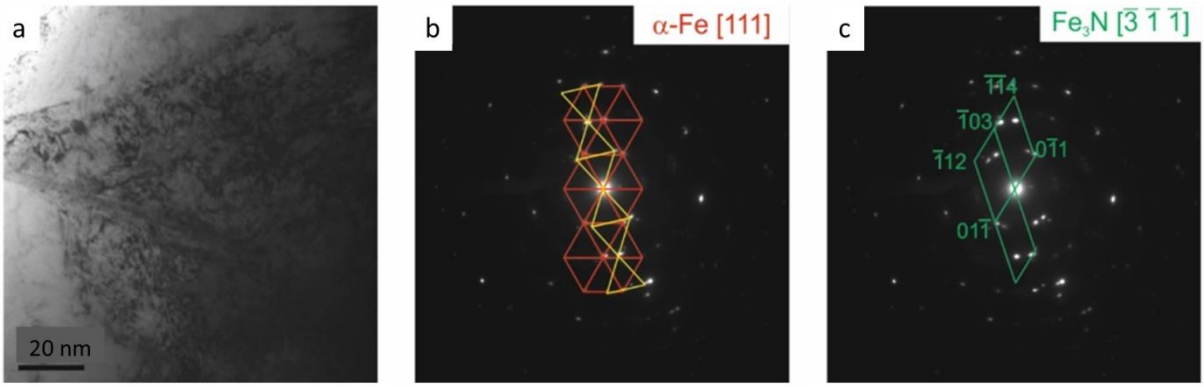

Figure 4. Electron microscopic images of stainless steel after high-intensity nitrogen ion implantation (at $T = 500$°C): a - bright-field image; b, c - microdiffraction pattern and schemes of their indexing.

The analysis of the diffractograms of AISI 321 steel samples implanted with nitrogen ions after electron-beam treatment (energy density 4 and 6 J/cm^2) showed that their surface layer has a pronounced crystal structure consisting of austenite γ-Fe and particles of chromium nitride CrN. In this case, the volume fraction of the γ-phase in the center of the modified sample after electron-beam

treatment at an energy density of 4 J/cm^2 is 93.9 wt.%, and chromium nitride CrN is 6.1 wt.%. With an increase in the electron beam energy density in a pulse to 6 J/cm^2, a change in the ratio of the phases formed in the surface layers of the implanted steel sample is observed: the volume fraction of the γ-phase is 98.2 wt.%, and chromium nitride CrN is 1.08 wt.%.

Figures 5 and 6 show the results of electron microscopic studies of the microstructure and phase composition of a stainless steel sample implanted with nitrogen ions in a cross-section after electron-beam treatment at an energy density of 4 and 6 J/cm^2, respectively.

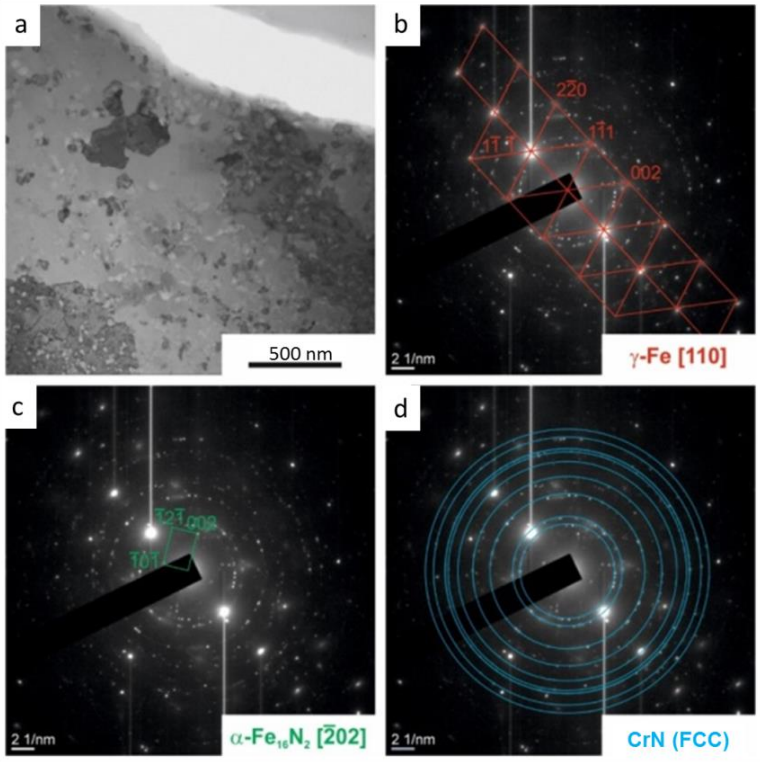

Figure 5. Electron-microscopic images of the cross-section of the implanted (at T = 500°C) sample of AISI 321 steel (surface) after electron-beam treatment with an energy density of 4 J/cm^2: a - bright field image; b, c and d - microdiffraction patterns and their indication schemes.

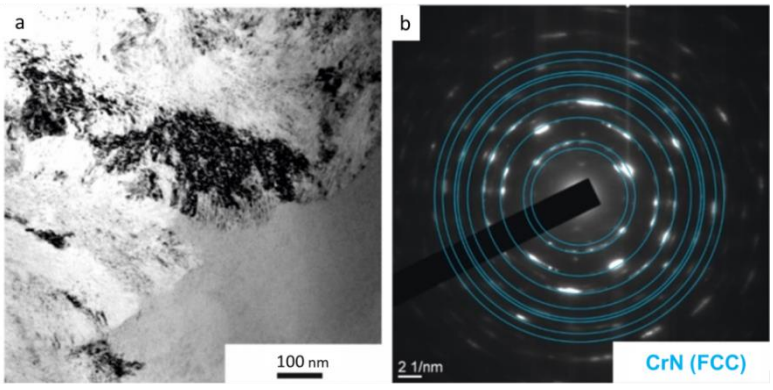

Figure 6. Electron-microscopic images of the cross section of the implanted (at T = 500°C) sample of AISI 321 steel (surface) after electron-beam treatment with an energy density of 6 J/cm^2: a - bright field image; b, c and d - microdiffraction patterns and their indication schemes

Analysis of bright-field electron microscopic images showed that electron-beam treatment of AISI 321 steel samples forms a modified layer on its surface, the thickness of which is determined by the electron beam energy density. So, as a result of pulsed electron-beam treatment with an energy density of 4 J/cm^2, the modified layer's thickness is about 20 μm, while when the energy density is 6 J/cm^2, the modified layer thickness is 7.5 μm. We assume that the decrease in the modified layer's thickness observed in the case of electron-beam treatment with an energy density in the pulse of 6 J/cm^2 is due to the process of intense material's evaporation from the surface of the AISI 321 steel

sample under study. The microdiffraction patterns obtained from the modified sample's surface layers (figure 5, b-d and 6, b) have a quasi-ring shape. As a result of microdiffraction patterns' identification (figure 6, b), it was found that CrN particles in the bulk of γ-Fe grains are formed in the implanted stainless steel sample's surface layer after electron-beam treatment. In addition, in the implanted surface layers of AISI 321 steel after electron-beam treatment with an energy density of 4 J/cm^2, in addition to the above phases, the formation of a metastable phase α''-$Fe_{16}N_2$ was found.

4. Conclusion

High-intensity implantation of AISI 321 stainless steel samples by a nitrogen ion beam in a system with ballistic focusing forms a two-layer structure consisting of a base nitride layer (Fe_3N), nitrides of alloying additives (mainly chromium), and a region of a nitrogen solid solution in the substrate material. According to the X-ray structural analysis it was found that the surface layers are characterized by a crystal structure and contain two phases: α-Fe (BCC) and high nitrogen iron nitride ε-Fe_3N (FCC). At that, the volume fraction of the α-phase is 79.4 wt.%, and the γ-phase is 20.6 wt.%. The obtained values of the CSR sizes for the formed high-nitrogen iron nitride indicate a very high dispersion of the substructure elements. Analyzing the diffractograms of post-implantation impact on the ion-doped layer of a high-current electron beam with sub-millisecond duration with energy densities of 4 and 6 J/cm^2 showed that their surface layer has a pronounced crystal structure, consisting of austenite γ-Fe and CrN chromium nitride particles. In this case, the volume fraction of the γ-phase at an electron beam energy density of 4 J/cm^2 is 93.9 wt.%, and chromium nitride CrN is 6.1 wt.%. With an increase in the energy density of the electron beam in the pulse to 6 J/cm^2, a change in the phases' ratio formed in the surface layers of the implanted steel sample is observed: the volume fraction of the γ-phase is 98.2 wt.%, and chromium nitride CrN is 1.08 wt.%.

Acknowledgments

This work was carried out with the financial support of the Russian Science Foundation (grant No. 17-19-01169 P).

References

[1] Yang Yang, Yan M F, Zhang S D, Guo J H, Jiang S S and Li D Y 2018 Diffusion behavior of carbon and its hardening effect on plasma carburized M50NiL steel: Influences of treatment temperature and duration *Surf. Coat. Tech.* **333** 96–103

[2] El-Hossary F M, Negm N Z, Khalil S M, Abed Elrahman A M and McIlroy D N 2001 RF plasma carbonitriding of AISI 304 austenitic stainless steel *Surf. Coat. Tech.* **141**(2-3) 194-201

[3] Goncharenko I M, Grigoriev S V, Lopatin I V, Koval N N, Schanin P M, Tukhfatullin A A, Ivanov Y F and Strumilova N V 2003 Surface modification of steels by complex diffusion saturation in low pressure arc discharge *Surf. Coat. Tech.* **169-170** 419-23

[4] Avelar-Batista J C, Spain E, Housden J, Matthews A and Fuentes G G 2005 Plasma nitriding of Ti6Al4V alloy and AISI M2 steel substrates using D.C. glow discharges under a triode configuration *Surf. Coat. Tech.* **200**(5-6) 1954-61

[5] Devyatkov V N, Ivanov Y F, Krysina O V, Koval N N, Petrikova E A and Shugurov V V 2017 Equipment and processes of vacuum electron-ion plasma surface engineering *Vacuum* **143** 464-72

[6] Escalada L, Lutz J, Brühl S P, Fazio M, Márquez A, Mändl S, Manova D and Simison S N 2013 Microstructure and corrosion behavior of AISI 316L duplex treated by means of ion nitriding and plasma based ion implantation and deposition *Surf. Coat. Tech.* **223** 41-6

[7] Rolin´ski E 2015 *Plasma-assisted nitriding and nitrocarburizing of steel and other ferrous alloys*. Chapter 11 in book: *Thermochemical Surface Engineering of Steels*, ed. Eric J. Mittemeijer and Marcel A.J. Somers, (Cambridge: Elsevier Ltd.)

[8] Wei R 1996 Low energy, high current density ion implantation of materials at elevated

temperatures for tribological applications *Surf. Coat. Tech.* **83**(1-3) 218-27
[9] Koval N N, Ryabchikov A I, Sivin D O, Lopatin I V, Krysina O V, Akhmadeev Y H and Ignatov D Y 2018 Low-energy high-current plasma immersion implantation of nitrogen ions in plasma of non-self-sustained arc discharge with thermionic and hollow cathodes *Surf. Coat. Tech.* **340** 152-8
[10] Ryabchikov A I, Sivin D O, Korneva O S, Ananyin P S, Ivanova A I and Stepanov I B 2019 Plasma-immersion formation of high-intensity gaseous ion beams *Vacuum* **165** 127-33
[11] Ryabchikov A I, Shevelev A E, Sivin D O, Ivanova A I and Medvedev V N 2018 Low energy, high intensity metal ion implantation method for deep dopant containing layer formation *Surf. Coat. Tech.* **355** 123-8
[12] Ryabchikov A I, Sivin D O, Ananin P S, Ivanova A I, Lopatin I V, Korneva O S and Shevelev A E 2018 High intensity, low ion energy implantation of nitrogen in AISI 5140 alloy steel *Surf. Coat. Tech.* **355** 129-35
[13] Ryabchikov A I, Sivin D O, Korneva O S, Lopatin I V, Ananin P S, Prokopenko N A and Akhmadeev Y K 2018 High-current-density gas ion ribbon beam formation *Nucl. Instrum. Meth.* A **906** 56-60
[14] Krysina O V, Shugurov V V, Prokopenko N A, Petrikova E A, Tolkachev O S and Denisova Y A 2019 Synthesis of single-layer ZrN-coatings using vacuum-arc plasma-assisted deposition with plasma flow filtering *Rus. Phys. J.* **62** 848–53
[15] Devyatkov V N, Koval N N, Schanin P M, Grigoryev V P and Koval T V 2003 Generation and propagation of high-current low-energy electron beams *Laser Part. Beams* **21**(2) 243-8